Calcium- and Myristoyl-Dependent Properties of Guanylate Cyclase-Activating Protein-1 and Protein-2†

Ji-Young Hwang and Karl-Wilhelm Koch*

Institut für Biologische Informationsverarbeitung 1, Forschungszentrum Jülich, D-52425 Jülich, Germany

Received August 12, 2002; Revised Manuscript Received August 29, 2002

ABSTRACT: In visual transduction, guanylate cyclase-activating proteins (GCAPs) activate the membrane-bound guanylate cyclase 1 (ROS-GC1) to synthesize cGMP under conditions of low cytoplasmic $[Ca^{2+}]_{free}$. GCAPs are neuronal Ca^{2+}-binding proteins with three functional EF-hands and a consensus site for N-terminal myristoylation. GCAP-1 and GCAP-2 regulated ROS-GC1 activities differently. The myristoyl group in GCAP-1 had a strong influence on the Ca^{2+}-dependent regulation of ROS-GC1 (shift in IC_{50}). In contrast, myristoylation of GCAP-2 did not change the cyclase activation profile (no shift in IC_{50}). Thus, the myristoyl group controlled the Ca^{2+}-sensitivity of GCAP-1, but not that of GCAP-2. The myristoyl group restricted the accessibility of one cysteine in GCAP-1 and GCAP-2 observed by measuring the time-dependent thiol reactivity of cysteines. This shielding effect was not relieved when Ca^{2+} was buffered by EGTA. We applied surface plasmon resonance (SPR) spectroscopy to monitor the Ca^{2+}-dependent binding of myristoylated and nonmyristoylated GCAP-1 and GCAP-2 to immobilized phospholipid membranes. None of the GCAPs exhibited a Ca^{2+}−myristoyl switch as observed for recoverin. Thus, the myristoyl group controls the Ca^{2+}-sensitivity of GCAP-1 (not that of GCAP-2) by an allosteric mechanism, but this control step does not involve a myristoyl switch

Neuronal calcium-sensor (NCS)[1] proteins constitute a family of EF-hand Ca^{2+}-binding proteins with a heterogeneous expression in various nervous tissue. They are grouped into five subfamilies named frequenins, visinin-like proteins (VILIPs), Kv-channel-interacting proteins (KchIPs), recoverins, and guanylate cyclase-activating proteins (GCAPs) (*1, 2*). NCS proteins modulate rather diverse biological phenomena such as, for example, potassium channel inactivation, repression of transcription, neurotransmitter release, and second messenger homeostasis. Among NCS proteins, the GCAPs are probably best understood in their biological function (*3*−*7*). These small acidic Ca^{2+}-sensor proteins are specifically expressed in photoreceptor cells, where they regulate the membrane-bound photoreceptor-specific guanylate cyclases (ROS-GC1 and ROS-GC2) in a Ca^{2+}-dependent manner (*8*−*10*). ROS-GCs are activated at low free $[Ca^{2+}]$ and inhibited at high free $[Ca^{2+}]$. The cytoplasmic $[Ca^{2+}]$ in rod and cone photoreceptor cells changes dynamically depending on illumination. In a dark-adapted cell, the cytoplasmic $[Ca^{2+}]$ is high (500−600 nM) and decreases after illumination (50−100 nM). Changes in cytoplasmic $[Ca^{2+}]$ are sensed by Ca^{2+}-binding proteins, e.g., calmodulin, recoverin, and GCAPs, which control or modulate their target proteins in a Ca^{2+}-dependent way. These Ca^{2+}-dependent feedback reactions terminate the photoresponse of the cell, lead to replenishment of the exhausted cGMP pool and mediate the regulation of light sensitivity in the cell (*11*−*14*).

All subfamilies of NCS proteins except the KChIPs contain a consensus site for N-terminal acylation and in principle could target to membranes by an extruded acyl chain (mainly myristoyl). Extrusion of the myristoyl group can be triggered by GDP/GTP exchange, phosphorylation, or Ca^{2+} in a variety of signal transduction proteins (*15*−*18*). Recoverin, for example, exhibits a so-called Ca^{2+}−myristoyl switch (*19, 20*). In its Ca^{2+}-free state, the myristoyl group is buried in a hydrophobic cleft. It becomes exposed, when Ca^{2+} binds to recoverin, and induces a conformational change. Recoverin is anchored in the membrane by the exposed myristoyl group, where it inhibits rhodopsin kinase activity in vertebrate photoreceptor cells (*21, 22*).

Native GCAP-1 and GCAP-2 resemble recoverin as they are heterogeneously acylated (mainly myristoylated), but the biological role of this acylation is only poorly understood in GCAPs. GCAP-2 does not show a classical, i.e., recoverin-like, Ca^{2+}−myristoyl switch, and lack of the myristoyl group in GCAP-2 does not impair or change its regulatory features (*23*). In contrast, myristoylated peptides encompassing the N-terminal region of GCAP-1 can inhibit the GCAP-1-dependent activation of cyclase (*3, 24*). A nonmyristoylated fusion protein of GCAP-1 displayed a lower affinity for the

† This work was supported by a grant from the Deutsche Forschungsgemeinschaft to K.-W.K. (Ko948/5-3).

* Correspondence should be addressed to this author at the Institut für Biologische Informationsverarbeitung 1, Forschungszentrum Jülich, D-52425 Jülich, Germany. Tel: ++49-2461-61-3255; fax: ++49-2461-614216; e-mail: k.w.koch@fz-juelich.de.

[1] Abbreviations: ROS, rod outer segment(s); ROS-GC1, photoreceptor membrane guanylate cyclase; nonmyr-GCAP, nonmyristoylated form of guanylate cyclase-activating protein-1 or -2; myr-D^{6}S-GCAP-1, myristoylated mutant of GCAP-1; myr-GCAP-2, myristoylated form of GCAP-2; NCS, neuronal Ca^{2+}-sensor; Rh, rhodopsin; NMT, N-terminal myristoyl transferase; DTNB, 5,5′-dithiobis(2-nitrobenzoic acid); TNB, 5-thio-2-nitrobenzoic acid; SPR, surface plasmon resonance; HPLC, high-performance liquid chromatography; IPTG, isopropyl-β-D-thiogalactoside; VILIPs, visinin-like proteins; KChIP, Kv-channel interacting protein.

10.1021/bi026618y CCC: $22.00
Published on Web 09/28/2002

cyclase and a shift of its Ca^{2+}-sensitivity (*6*). In addition, the inhibition of ROS-GC1 at high [Ca^{2+}] requires the presence of the myristoyl group in GCAP-1 (*25*), but membranes are not necessary to mediate the effect (*26*). Thus, it appears that the myristoyl group is critical for the function of GCAP-1, but it is unclear how it affects the properties of GCAP-1. We investigated how the myristoyl group influences some key properties of GCAP-1 in comparison to GCAP-2. We tested, for example, regulatory properties using guanylate cyclase assays, membrane binding using surface plasmon resonance (SPR) spectroscopy, and possible Ca^{2+}-induced movements of the myristoyl moiety using absorption spectroscopy of thiol modification.

MATERIALS AND METHODS

Expression of GCAPs. GCAPs were expressed in *Escherichia coli* as described (*24*). For the myristoylation of the N-terminus of GCAPs, the plasmid pBB-131 was used. This plasmid contains N-terminal myristoyl transferase 1 (NMT1) from *Saccharomyces cerevisiae*, kindly provided by Dr. J. I. Gordon.

Plasmid pET-11a/GCAP was constructed by subcloning DNA fragments with the GCAP1, D^6S-GCAP1, and GCAP2 genes with *Nde*I/*Bam*HI into the vector pET-11a. D^6S-GCAP-1 is a point mutant of GCAP-1, wherein substitution of aspartate by serine at position 6 creates a myristoylation consensus site for yeast N-terminal myristoyl transferase 1 (*27*).

Bacterial strains Epicurian Coli BL21-CodonPlus(DE3)-RIL (Stratagene) were used for overexpression of GCAPs. Cells were cultured in dYT medium at 37 °C. Myristic acid (100 μg/mL in ethanol) was added to the culture at an OD_{600} of 0.4. Expression of myristoylated GCAPs was induced by 1 mM IPTG at 37 °C. After 4 h, cells were harvested by centrifugation for 20 min at 10000*g* at 4 °C and then resuspended in 20 mM Tris, pH 7.4, 150 mM NaCl, 2 mM EGTA or 2 mM $CaCl_2$, 2 mM DTT, and proteinase inhibitor cocktail mix (Boehringer Mannheim, Germany).

Purification of GCAPs and Isolation of Myristoylated GCAPs. The overexpressed GCAPs were released from the BL21-CodonPlus(DE3)-RIL cells by passing through a French press (SLM Aminco). Subsequent purification of GCAPs by size exclusion and anion exchange chromatography using an ÄKTA FPLC system (Pharmacia Biotech, Sweden) was exactly as described (*28*). Purified GCAPs were dialyzed against 50 mM ammonium bicarbonate buffer. Aliquots of 1 mg were lyophilized by a Speedvac concentrator and then stored at −80 °C till further use.

Myristoylated forms of GCAP-1 or GCAP-2 were separated from the nonmyristoylated forms by reversed phase chromatography as described (*28*). Briefly, each sample was injected into a Vydac 238TP C18 reverse-phase column (4.6 × 250 mm) (Vydac) and eluted with a gradient of 0−80% (v/v) acetonitrile/0.1% (v/v) TFA at a flow rate of 1.0 mL/min. The elution was monitored by absorbance at 280 nm.

Preparation of Rod Outer Segment Membranes and Guanylate Cyclase Assay. Rod outer segments (ROS) were prepared from freshly collected bovine eyes as described before (*6, 24*).

Guanylate cyclase activities were determined with washed ROS membranes as a source for native ROS-GC1 (the amount of ROS-GC2 in our bovine ROS preparation is less than 5% of the ROS-GC1; Hwang et al., in preparation). Washed ROS membranes were prepared by diluting ROS 5-fold with washing buffer (10 mM Hepes-KOH, pH 7.4, 1 mM DTT) and centrifugation for 10 min at 80 000 rpm in a Beckman TLA100 centrifuge at 4 °C. The washing procedure was repeated. The resulting pellet was resuspended in half of the original ROS volume in resuspension buffer (50 mM Hepes-KOH, pH 7.4, 500 mM KCl, 20 mM NaCl, 1 mM DTT). Ten microliters of GCAPs (2 μM) was added to 10 μL of washed ROS membranes to give a total volume of 20 μL. Those reaction samples were preincubated for 5 min at room temperature with 10 μL of Ca^{2+}/EGTA buffer of varying free [Ca^{2+}]. Ca^{2+}/EGTA buffer solutions were prepared as described by Tsien and Pozzan (*29*). Free [Ca^{2+}] was calculated with the Ca^{2+}-buffer program CHELATOR (*30*) using the constants of Martell and Smith (*31*). The cyclase reaction was started by adding 20 μL of Mg^{2+}/GC buffer (100 mM MOPS, pH 7.1, 140 mM KCl, 20 mM NaCl, 25 mM $MgCl_2$, 5 mM GTP) containing ATP and the PDE inhibitor zaprinast. Final concentrations of ATP and the PDE inhibitor zaprinast (Sigma) were 100 μM and 0.4 mM, respectively. The resulting suspension containing GCAPs and ROS membranes was incubated for 5 min at 30 °C. The incubation was stopped by adding ice-cold 50 mM EDTA and boiling for 5 min.

The activity of ROS-GC1 was determined by a HPLC chromatography assay using a nucleotide separation protocol as described before (*28*). Afterward the solution was centrifuged for 5 min at 13 000 rpm in a microcentrifuge. The supernatants (≤95 μL) were injected into an HPLC reversed-phase C18 column (4 × 250 mm) (Merck, Germany), and nucleotides were eluted with a gradient of 0−70% (v/v) methanol in 5 mM KH_2PO_4, pH 5.0, at a flow rate of 1.2 mL/min. The elution was monitored by absorbance at 254 nm.

The activity unit is nmol of cGMP × min^{-1} × (mg of Rh)$^{-1}$. The data were fitted by the modified Hill equation using the program ORIGIN 6.1 (Microcal Software Inc., Northhampton, MA): $V/V_{max} = 1 - (Z \times [Ca^{2+}]^n)/([Ca^{2+}]^n + IC_{50}{}^n)$, where V is the activity of ROS-GC1, V_{max} is the maximal activity of ROS-GC1, n is the Hill coefficient, IC_{50} is the half-maximal value of Ca^{2+}-dependent ROS-GC1 activation, and Z is a constant taking into account that ROS-GC1 activity is not zero at high free [Ca^{2+}].

Surface Plasmon Resonance (SPR) Measurements. Binding of GCAPs to lipid membranes was tested by SPR spectroscopy using the BIAcore technology (BIAcore, Sweden). A mixture of 2 mg of lipids [40% (w/w) L-α-phosphatidylethanolamine (PE), 40% (w/w) L-α-phosphatidylcholine (PC), 15% (w/w) L-α-phosphatidylserine (PS), 5% (w/w) cholesterol] in CH_3Cl corresponding to the lipid composition in bovine ROS membranes (*32*) was lyophilized by a Speed Vac concentrator. The sample was resuspended in 1 mL of 10 mM Hepes, pH 7.4, 150 mM KCl, 2 mM EGTA and sonicated at 100 W for 10 min 2 times using a Brandson B12 sonifier. The suspension was soaked for an hour and extruded several times through the PC polycarbonate filters (Corning) with pore diameters of 1 and 0.4 μm. Injection of recoverin was used as a positive control (*33*).

Liposomes were immobilized on a Pioneer L1 sensor chip (BIAcore, Sweden) with 10 mM Hepes, pH 7.4, 150 mM

KCl, 20 mM $MgCl_2$, 2 mM $CaCl_2$ as running buffer. Pioneer Chip L1 has a carboxymethylated dextran matrix that has been modified with lipophilic substances, allowing work with bilayers. Interaction of GCAPs with lipid membranes was tested by application of 3 μM GCAPs in 10 mM Hepes, pH 7.4, 150 mM KCl, 20 mM $MgCl_2$, 2 mM $CaCl_2$ or 2 mM EGTA. The flow rate was 5 μL/min. Nonspecific binding to membranes was probed by injection of protein G (control recording).

Thiol Reactivity of GCAPs. Quantitative determination of thiol groups in solution was performed by recording the formation of 5-thio-2-nitrobenzoic acid (TNB) from 5,5′-dithiobis(2-nitrobenzoic acid) (DTNB) at 412 nm as described (*34*). A fresh solution of DTNB (12.5 mM) was prepared by dissolving it in 0.1 M Tris, pH 8.0, and sonicating for 1 min at 80−100 W. Thiol reactivity of GCAPs was measured by the addition of 100 μM DTNB into a cuvette containing 0.5 μM GCAPs in 50 mM Hepes, pH 7.4, 100 mM NaCl and either 100 μM $CaCl_2$ or 2 mM EGTA. The time course of TNB formation at 412 nm was recorded after injection of DTNB using a Shimadzu UV-2101PC UV/VIS scanning spectrophotometer (Shimadzu, Japan). When samples were preincubated with $CaCl_2$, EGTA was injected 5 min after application of DTNB. In a second set of experiments, the order of $CaCl_2$ and EGTA application was reversed ($CaCl_2$ in excess). The number of reactive cysteines can be calculated from a calibration curve according to: $A_{412} = 0.015 + (0.014 \times [\text{thiol}]_{\text{free}})$ using cysteine standard solutions (*34*).

RESULTS

Myristoylated D^{6}S-GCAP-1 and GCAP-2 were purified from *E. coli* cell extracts with high yields (10−50 mg/L). The D^{6}S mutation was introduced into GCAP-1 to facilitate myristoylation by yeast NMT in *E. coli* (*27*). We verified the attachment of the myristoyl group by HPLC analysis on a reversed-phase column (*28*). GCAPs undergo a Ca^{2+}-induced conformational change, which can be monitored by a gel shift assay (*3*−*7*). The electrophoretic mobility is higher in the presence of Ca^{2+} and lower in the presence of EGTA. We applied this shift assay to all four proteins (myr-D^{6}S-GCAP-1, nonmyr-GCAP-1, myr-GCAP-2, and nonmyr-GCAP-2 in Figure 1A). The extent of this shift was determined from a plot of the relative mobility as a function of the molecular mass using molecular weight standards to create a calibration curve (Figure 1B). Purified myristoylated GCAPs exhibited an electrophoretic mobility shift of 4.8−4.9 kDa, nonmyristoylated GCAPs of 4.5 kDa (Figure 1 and Table 1). These results indicate that a similar Ca^{2+}-induced conformational change occurs in the myristoylated and nonmyristoylated forms of GCAPs. However, the shift was slightly larger (4.8−4.9 versus 4.5 kDa) when the myristoyl group was present. This might reflect subtle differences in hydrodynamic shape or conformation between nonmyristoylated and myristoylated forms.

Regulation of Guanylate Cyclase Activity. GCAPs operate in visual cells as Ca^{2+}-sensitive regulators of membrane-bound guanylate cyclases (ROS-GC1 and ROS-GC2). We used native bovine ROS membranes to test the influence of the myristoyl group on the activation of ROS-GC1 by GCAPs (more than 95% of the two guanylate cyclases in bovine ROS membranes is ROS-GC1; see also Materials and Methods). Samples were incubated in the presence and absence of 2 μM GCAP-1 or GCAP-2 forms and varying $[Ca^{2+}]_{\text{free}}$ (Figure 2 and Table 2). The maximal activity of ROS-GC1 at low $[Ca^{2+}]_{\text{free}}$ was higher, when the myristoyl group was attached. In addition, the *x*-fold activation (i.e., the ratio of cyclase activity at low and high $[Ca^{2+}]$ in the presence of GCAPs) was also higher, when the myristoyl group was present. Although nonmyr-GCAP-2 exhibited a

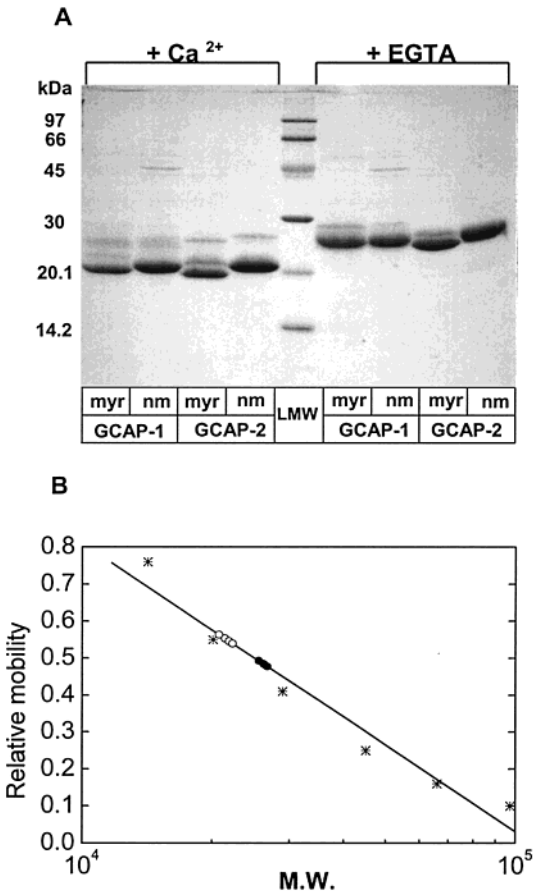

FIGURE 1: Electrophoretic mobilities of GCAPs. (A) Purified myristoylated (myr) and nonmyristoylated (nm) GCAPs exhibited an electrophoretic mobility shift in a 15% SDS−PAGE, when $CaCl_2$ was replaced by EGTA. The myristoylated D^{6}S-mutant of GCAP-1 was used. The faint band above myr-GCAP-2 represents nonmyr-GCAP-2. (B) A calibration curve of molecular weight standards created from plotting the relative mobility (R_f) of standards versus their molecular mass (M.W.). Standards were phosphorylase *b* (97.4 kDa), bovine serum albumin (66 kDa), ovalbumin (45 kDa), carbonic anhydrase (29 kDa), soybean trypsin inhibitor (20.1 kDa), and α-lactalbumin (14.2 kDa). R_f-values of GCAPs in the presence of $CaCl_2$ (open circles) or EGTA (closed circles) are located on the linear slope of the plot. The corresponding values of the exact apparent MW are listed in Table 1.

Table 1: Comparison of Relative Electrophoretic Mobility and Apparent Molecular Weight of myr-D^{6}S-GCAP-1, nonmyr-GCAP-1, myr-GCAP-2, and nonmyr-GCAP-2 by SDS−PAGE Analysis

type	theoretical MW (kDa)	apparent MW (kDa) with EGTA	apparent MW (kDa) with Ca^{2+}	ΔMW(EGTA-Ca^{2+}) (kDa)
myr-D^{6}S-GCAP-1	23.6	26.2	21.4	4.8
nonmyr-GCAP-1	23.4	26.4	21.9	4.5
myr-GCAP-2	23.8	25.6	20.7	4.9
nonmyr-GCAP-2	23.6	26.8	22.3	4.5

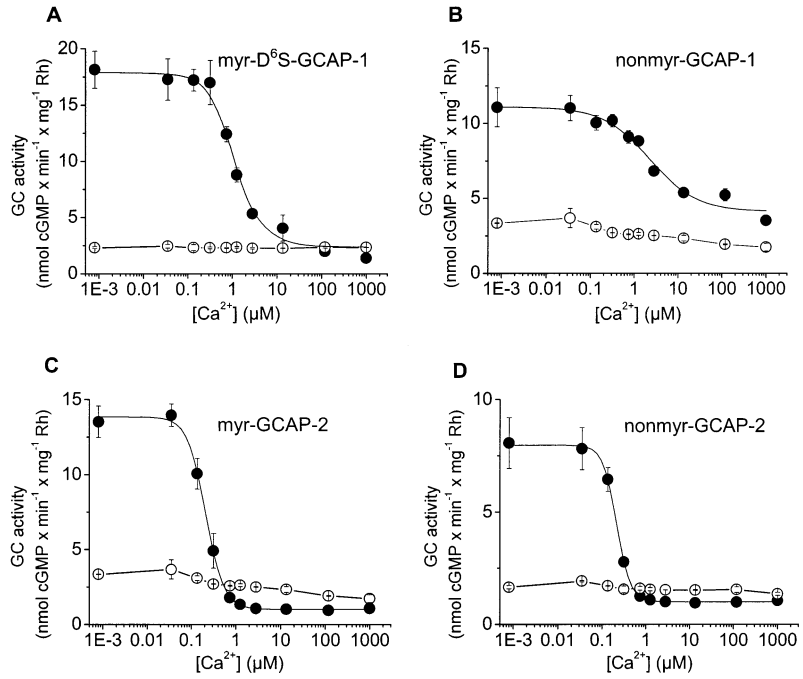

FIGURE 2: Regulation of ROS-GC1 by GCAPs. Washed bovine ROS membranes containing ROS-GC1 were reconstituted with 2 μM GCAPs at varying $[Ca^{2+}]_{free}$ (closed circles). Control incubations (open circles) were without added GCAPs. (A) myr-D^{6}S-GCAP-1; (B) nonmyr-GCAP-1; (C) myr-GCAP-2; and (D) nonmyr-GCAP-2.

Table 2: Regulation of ROS-GC1 by GCAPs[a]

type	maximal activity	*x*-fold activation	$IC_{50}[Ca^{2+}]_{free}$ (μM)	*n*, Hill coefficient
myr-D^{6}S-GCAP-1	17.90 ± 0.56	9	1.088 ± 0.129	1.7
nonmyr-GCAP-1	11.11 ± 0.41	3	2.240 ± 0.776	0.8
myr-GCAP-2	13.85 ± 0.18	14	0.209 ± 0.007	2.4
nonmyr-GCAP-2	7.97 ± 0.05	9	0.214 ± 0.004	2.7

[a] Activity is expressed as nmol of cGMP × min^{-1} × (mg of Rh)$^{-1}$.

lower maximal activity than nonmyr-GCAP-1 [7.97 versus 11.11 nmol of cGMP × min^{-1} (mg of Rh)$^{-1}$], the *x*-fold activation was 3 times higher in the case of nonmyr-GCAP-2 (Figure 2 and Table 2). This is mainly due to a stronger inhibitory effect of GCAP-2 at high $[Ca^{2+}]$ ($\geq$1 μM in Figure 2), which is clearly visible with myristoylated and nonmyristoylated GCAP-2 (Figure 2C,D) and only slightly apparent with myr-D^{6}S-GCAP-1 (see data points $\geq$100 μM $[Ca^{2+}]$ in Figure 2A), but it was not observed with nonmyr-GCAP-1 (Figure 2B).

One hallmark of GCAP function is the cooperative activation of ROS-GCs, when $[Ca^{2+}]_{free}$ decreases (*3*−*10*). Myristoylation did not change the activation profile of GCAP-2; for example, the half-maximal activation (IC_{50}) and Hill coefficients (*n*) were very similar (Table 2) for myristoylated and nonmyristoylated GCAP-2. However, the myristoyl group in GCAP-1 had a strong influence on the Ca^{2+}-dependent regulation of ROS-GC1. Lack of myristoylation caused a 2-fold shift of the IC_{50} value and a complete loss of cooperativity (Figure 2A,B, Table 2). We conclude from these results that the myristoyl group controls the Ca^{2+}-sensitivity of GCAP-1, but not that of GCAP-2.

Interaction of GCAPs with Membranes Monitored by SPR Spectroscopy. Some NCS proteins such as recoverin exhibit a Ca^{2+}−myristoyl switch, i.e., a Ca^{2+}-dependent association of the protein with membranes (*1*, *2*). The myristoyl group serves as an anchor to tether the protein to the surface of the membrane. SPR spectroscopy was previously used to investigate the dynamics of the Ca^{2+}−myristoyl switch of recoverin (*33*) and neurocalcin (*35*). We here used a similar approach to study the membrane association of GCAP-1 and GCAP-2 forms. Phospholipids were immobilized on a sensor chip surface. These immobilized lipid layers were sufficiently stable to allow the recording of binding signals. Protein samples were injected into the flow cell of the system (BIAcore), and changes in resonance units were recorded as a function of time to yield sensorgrams as shown in Figure 3. We recorded the binding of proteins in the presence of either Ca^{2+} or EGTA. Myristoylated recoverin served as positive control, because its Ca^{2+}−myristoyl switch is well documented and can be monitored by SPR spectroscopy (*33*). Protein G was injected to measure any nonspecific association of a protein with membranes and to determine changes in bulk refractive index. The Ca^{2+}−myristoyl switch of recoverin is manifest as a large amplitude of the SPR signal in the presence of Ca^{2+} and a small amplitude in the presence of EGTA. Binding signals of recoverin obtained in the presence of EGTA had a slightly higher amplitude than the control recordings with protein G (Figure 4A). In contrast, sensorgrams obtained with GCAP-1 and GCAP-2 exhibited several significant differences when compared with control recordings (Figures 3 and 4). Amplitudes recorded 7 min after injection (black bar in Figure 3 indicates injection of protein) were similar in sensorgrams with myrD^{6}S-GCAP-1, nonmyr-GCAP-1, and nonmyr-GCAP-2, no matter whether Ca^{2+} or EGTA was present (Figures 3 and 4A).

Examples of sensorgrams in Figure 3 show higher amplitudes for myr-D^{6}S-GCAP-1, nonmyr-GCAP-1, and nonmyr-GCAP-2 in the presence of EGTA than in the presence of Ca^{2+}. However, recordings from at least four different experiments showed that these differences were not

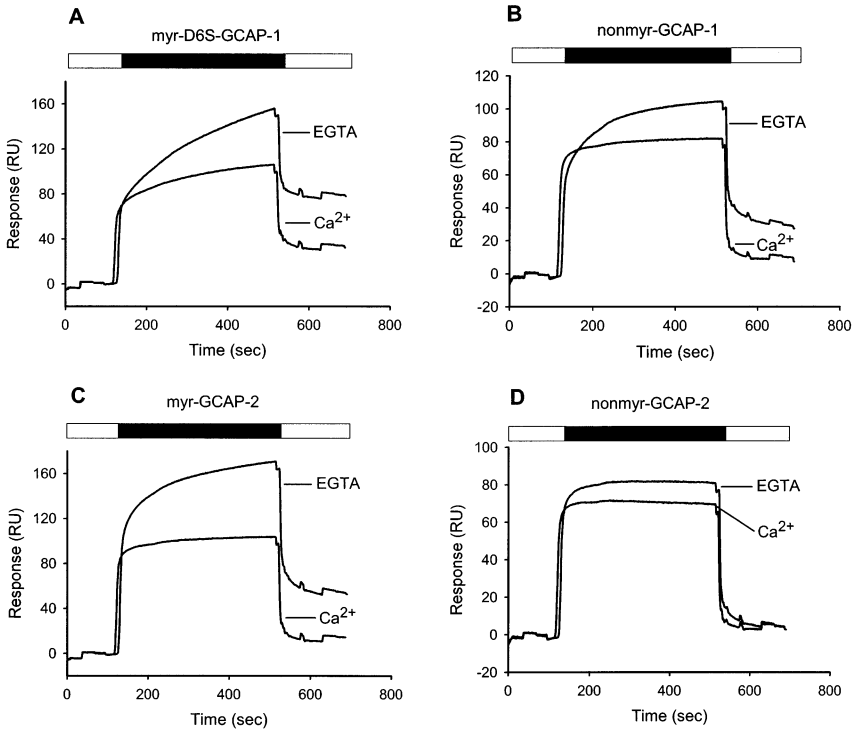

FIGURE 3: Binding of GCAPs to immobilized liposomes monitored by SPR spectroscopy. Liposomes were immobilized on a L1 sensor chip (BIAcore). GCAPs were suspended in SPR running buffer containing either $CaCl_2$ or EGTA and injected into the flow cell at a concentration of 3 μM (black bar). Running buffer (open bar) was the same before and after injection and contained either $CaCl_2$ or EGTA. Recordings were obtained with myr-D^{6}S-GCAP-1 (A), nonmyr-GCAP-1 (B), myr-GCAP-2 (C), and nonmyr-GCAP-2 (D).

statistically significant (Figure 4). Interestingly, myr-GCAP-2 always showed a larger amplitude in the presence of EGTA (Figures 3 and 4A), which is consistent with a previous observation by Olshevskaya et al. (*23*) that GCAP-2 associates with ROS membranes at low free [Ca^{2+}] and is released from membranes at high [Ca^{2+}]. Furthermore, it is noticeable that recordings in the presence of EGTA were higher with GCAPs than with recoverin (Figure 4A).

A summary of these data is shown in Figure 4B; amplitudes recorded in the presence of Ca^{2+} ($RU_{Ca^{2+}}$) were divided by the amplitudes recorded in the presence of EGTA (RU_{EGTA}). Values above 1 show the working of a Ca^{2+}−myristoyl switch (myristoylated recoverin as positive control), and values around 1 indicate no operation of this switch. Thus, we conclude that GCAP-1 and GCAP-2 do not perform a classical Ca^{2+}−myristoyl switch as recoverin.

Thiol Reactivity of Cysteines in GCAPs. GCAP-1 and GCAP-2 contain four and three cysteines, respectively. The four cysteines in GCAP-1 are accessible to the thiol-modifying reagent DTNB, but the accessibility of one cysteine (C106) depends on the complete chelation of Ca^{2+} (*34*). We tested whether the thiol reactivities of cysteines in GCAP-1 and GCAP-2 depend on Ca^{2+} and the presence of the myristoyl group. Reaction of DTNB with free thiol groups leads to an increase in the absorbance at 412 nm. When nonmyr-GCAP-1 was preincubated with 100 μM $CaCl_2$, injection of DTNB caused a change in absorbance at 412 nm that corresponds to the modification of three cysteines (trace 1 in Figure 5A). Injection of EGTA then triggered an additional reaction of DTNB with the fourth cysteine (arrow pointing to trace 1 in Figure 5A). When nonmyr-GCAP-1 was first incubated with EGTA, DTNB reacted immediately with all four cysteines (trace 2 in Figure 5A). However, in myr-D^{6}S-GCAP-1 only two cysteines reacted with DTNB in the presence of Ca^{2+}, and addition of EGTA caused the exposition of one additional cysteine (trace 1 in Figure 5B). Reversing the injection of Ca^{2+} and EGTA led to the modification of three cysteines. Thus, when GCAP-1 was myristoylated, one cysteine did not react with DTNB.

Injection of DTNB into a solution of nonmyr-GCAP-2 caused a reaction with all three cysteines (Figure 5C). Reversing the order of Ca^{2+} and EGTA addition (trace 2 in Figure 5C) yielded a nearly identical recording. When we used myr-GCAP-2, only two cysteines were accessible to DTNB. One cysteine did not react with DTNB irrespective of the order of Ca^{2+} and EGTA addition (Figure 5D). We conclude from these results that the myristoyl group has a strong shielding effect in GCAP-1 and GCAP-2. This shielding effect is not relieved when the [Ca^{2+}] is changed.

DISCUSSION

GCAP-1 and GCAP-2 undergo a major conformational change upon binding of Ca^{2+}. Limited proteolysis of Ca^{2+}-bound GCAP-1 by trypsin cleaves off the myristoylated N-terminus and the C-terminus, but leaves most of the protein intact. The Ca^{2+}-free form is more vulnerable to proteolysis and degraded to smaller fragments (*36*). Tryptophan fluorescence spectroscopy had shown that this conformational change occurs around EF-hand 3 (*37*). GCAP-2 also changes its conformation by binding of Ca^{2+} as revealed by UV−CD and NMR spectroscopy, and its myristoylated N-terminus is solvent-exposed in the Ca^{2+}-bound and Ca^{2+}-free states (*38*). Thus, in both proteins, the myristoyl group is probably not sequestered into a hydrophobic pocket when Ca^{2+} is absent and extruded when Ca^{2+} is bound, as described for

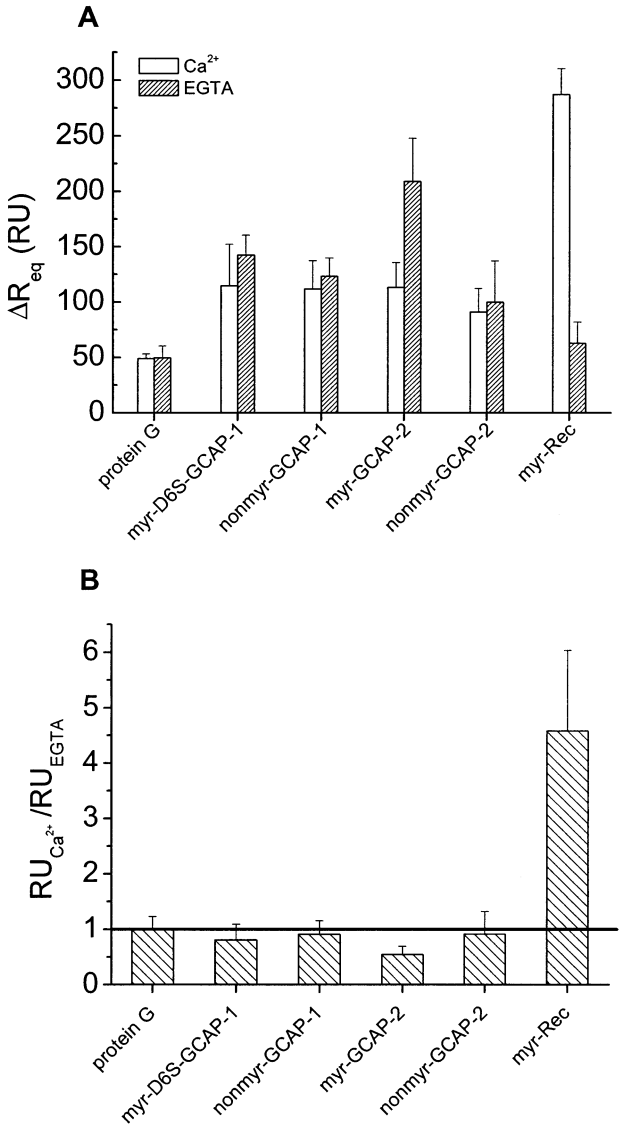

FIGURE 4: Amplitudes of SPR signals. (A) SPR resonance signals (ΔR_{eq}) were obtained by binding of proteins to lipid membranes in the presence of Ca^{2+} (blank columns) and in the presence of EGTA (striped columns). Control recordings were obtained with protein G. (B) Amplitudes of SPR resonance signals in the presence of Ca^{2+} were divided by the signal in the presence of EGTA. A ratio that was significantly higher than 1 was only observed with myristoylated recoverin (myr-Rec). Data are the mean ± SD of at least four recordings.

recoverin (*39*, *40*). So far, structural information of the exact location of the myristoyl group is lacking; only the three-dimensional structure of nonmyristoylated GCAP-2 has been resolved (*41*). The different accessibilities of free cysteines in myristoylated and nonmyristoylated GCAPs represent a new approach to investigate the location and dynamics of the myristoyl group. In both GCAPs, the myristoyl group exerts a shielding effect for one cysteine. Although both GCAPs undergo a conformational change upon binding of Ca^{2+} (see also Figure 1 and Table 1), this change does not cause a significant rearrangement of the myristoyl group, since the chemical reaction of one cysteine with DTNB is further prevented. However, the myristoyl group probably does not protect the particular cysteine from modification by direct interaction. Spectroscopic and proteolysis data indicate the permanent exposition of the myristoyl group to the solvent (*36*, *38*); thus, it might not be in direct vicinity of the corresponding cysteine. Therefore, it is tempting to speculate that the myristoyl group acts as an allosteric regulator of GCAPs that influences the Ca^{2+}-induced conformational change without participating in a structural change. Our data on the activation profiles of ROS-GC1 support this model for GCAP-1. The strong cooperative Ca^{2+}-dependent activation by myr-D^{6}S-GCAP1 (and also by native wild-type GCAP-1; see references *3*−*7*) was lost when nonmyr-GCAP-1 was assayed (Figure 2 and Table 2), indicating a loss of allostery. However, this was not observed for GCAP-2 and points to one of several significant differences between GCAP-1 and GCAP-2.

Exposition of the myristoyl group does not facilitate the binding to immobilized phospholipids (Figures 3 and 4), because we did not observe significant differences in amplitudes of SPR recordings between myristoylated and nonmyristoylated proteins (Figures 3 and 4A). Only myristoylated GCAP-2 showed stronger association with membranes in the absence of Ca^{2+}, but an "inverse Ca^{2+}−myristoyl switch" is probably not operating (*41*). Initial titration experiments indicated that the affinity of GCAPs for membranes is in the lower micromolar range (J.-Y. Hwang and K.-W. Koch, unpublished observation), which is expected for protein−membrane interaction driven by weak hydrophobic and a small contribution of electrostatic forces (*17*). The three-dimensional structure of Ca^{2+}-bound nonmyristoylated GCAP-2 shows a hydrophobic patch formed by residues from EF-hand 1 and EF-hand 2 (*41*). Since EF-hand 1 is required for targeting to photoreceptor guanylate cyclase (*42*), aromatic and aliphatic residues in EF-hand 2 could participate in membrane binding. In the Ca^{2+}-free state of myristoylated GCAP-2, hydrophobic and charged residues might become more exposed and increase the binding affinity for membranes.

We noticed that dissociation of GCAPs from immobilized membranes contained a slower component in the presence of EGTA (Figure 3); however, with nonmyr-GCAP-2 this was not visible. In our test system, immobilized phospholipids and soluble GCAPs, this observation indicates a more efficient tethering of Ca^{2+}-free GCAPs to the lipid layer. However, we did not apply a full quantitative evaluation to this effect, because the dissociation and association phases seemed to depend on a variety of factors and did not show exactly the same profiles in different recordings. Therefore, we restricted the quantitative evaluation of sensorgrams (Figure 4) to the amplitudes. A reliable descripton of the kinetic processes will be the focus of a future study.

A striking difference between GCAP-1 and GCAP-2 was also observed in activation of ROS-GC1 (Figure 2 and Table 2). The myristoyl group had a stronger influence on the properties of GCAP-1 than of GCAP-2. In particular, the Ca^{2+}-sensitivity of GCAP-1, but not that of GCAP-2, is controlled by an attached myristoyl group. A shift in the Ca^{2+}-sensitivity was previously observed for a fusion construct of GCAP-1 that contained a short sequence of six amino acids instead of a myristoyl group at the N-terminus (*6*). Thus, a peptide extension of the N-terminus appears to mimic the effect of the myristoyl group. Nonmyristoylated GCAP-1 was less active at low [Ca^{2+}], but at high [Ca^{2+}], inhibition of ROS-GC1 was also lower than with myr-D^{6}S-GCAP-1 (Figure 2B and Table 2). A similar effect was

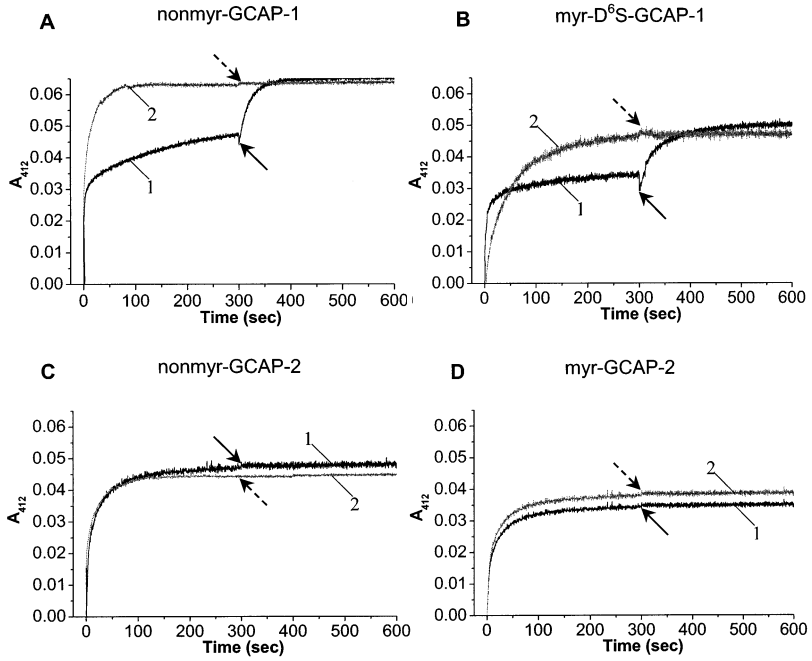

FIGURE 5: Cysteine reaction of GCAPs with DTNB. Time course of thiol reactivity was measured at 412 nm (formation of TNB). Traces labeled with 1: GCAPs (0.4−0.6 μM) were preincubated with 100 μM $CaCl_2$, and reaction was started by injection of 100 μM DTNB. After 300 s, 2 mM EGTA was injected (see arrow), and the response was recorded for 300 s. Traces labeled with 2: Order of $CaCl_2$ and EGTA application was reversed. Arrows indicate injection of $CaCl_2$. (A) nonmyr-GCAP-1; (B) myr-D^{6}S-GCAP-1; (C) nonmyr-GCAP-2; and (D) myr-GCAP-2.

observed with a truncated mutant of GCAP-1 that lacked the first 10 amino acids at the N-terminus (*25*). Thus, the Ca^{2+}-induced "activator to inhibitor" transition of GCAP-1 is promoted by the myristoyl group. Although this transition works even more powerful in GCAP-2 (*43*), the myristoyl group did not affect this transition in GCAP-2.

Recently, Mendez et al. (*44*) had shown that transgenic mice lacking expression of GCAP-1 and GCAP-2 had lost the Ca^{2+}-sensitivity of guanylate cyclase. Expression of GCAP-2 in these double knock-out mice restored the Ca^{2+}-sensitivity of cyclase. However, normal recovery kinetics of the flash response were only restored by expression of GCAP-1 (*45*), but not by expression of GCAP-2 (*44*). Our results on different Ca^{2+}-sensitivities of GCAPs (Table 2 and Figure 2A,C) indicate that GCAP-1 activates cyclase over a wider range of free [Ca^{2+}] than GCAP-2 does. GCAP-1 is switched on, when the cytoplasmic [Ca^{2+}] starts falling from its high dark value. GCAP-1 would therefore significantly participate in shaping the early rapid phase of the recovery kinetics of a flash response as observed by Howes et al. (*45*). In this model, GCAP-2 is switched on (Figure 2C), when [Ca^{2+}] has fallen to a lower steady-state value (>200 nM). GCAP-2 activates ROS-GC1 to a similar maximal activity as GCAP-1 does, which is consistent with the observation that expressison of GCAP-2 on a GCAP double knock-out background can restore maximal light-induced guanylate cyclase activity (*44*).

In summary, we have shown that GCAP-1 and GCAP-2 differ in their use of an attached myristoyl group. Recent findings on other NCS proteins such as hippocalcin, NCS-1, and neurocalcin δ have demonstrated that closely related Ca^{2+}-sensor proteins can use their myristoyl groups in different ways (*46*). This is rather surprising, since the known three-dimensional structures of some NCS proteins (*41*, *47*, *48*) resemble in their overall fold the structure of recoverin (*39*, *40*). Therefore one would expect a similar Ca^{2+}−myristoyl switch as a trigger for translocation to the membrane. However, the opposite seems to be true; the myristoyl group fulfills a specific task in each NCS protein.

ACKNOWLEDGMENT

We thank D. Höppner-Heitmann for excellent technical assistence.

REFERENCES

1. Braunewell, K.-H., and Gundelfinger, E. D. (1999) *Cell Tissue Res. 295*, 1−12.
2. Burgoyne, R. D., and Weiss, J. L. (2001) *Biochem. J. 353*, 1−12.
3. Palczewski, K., Subbaraya, I., Gorczyca, W. A., Helekar, B. S., Ruiz, C. C., Ohguro, H., Huang, J., Zhao, X., Crabb, J. W., Johnson, R. S., Walsh, K. A., Gray-Keller, M. P., Detwiler, P. B., and Baehr, W. (1994) *Neuron 13*, 395−404.
4. Gorczyca, W. A., Polans, A. S., Surgucheva, I. G., Subbaraya, I., Baehr, W., and Palczewski, K. (1995) *J. Biol. Chem. 270*, 22029−22036.
5. Dizhoor, A. M., Olshevskaya, E. V., Henzel, W. J., Wong, S. C., Stults, J. T., Ankoudinova, I., and Hurley, J. B. (1995) *J. Biol. Chem. 270*, 25200−25206.
6. Frins, S., Bönigk, W., Müller, F., Kellner, R., and Koch, K.-W. (1996) *J. Biol. Chem. 271*, 8022−8027.
7. Haeseleer, F., Sokal, I., Li, N., Pettenati, M., Rao, N., Bronson, D., Wechter, R., Baehr, W., and Palczewski, K. (1999) *J. Biol. Chem. 274*, 6526−6535.
8. Dizhoor, A. M., and Hurley, J. B. (1999) *Methods 19*, 521−531.
9. Palczewski, K., Polans, A. S., Baehr, W., and Ames, J. B. (2000) *BioEssays 22*, 337−350.
10. Koch, K.-W., Duda, T., and Sharma, R. K. (2002) *Mol. Cell. Biochem. 230*, 97−106.
11. Pugh, E. N., Jr., Nikonov, S., and Lamb, T. D. (1999) *Curr. Opin. Neurobiol. 9*, 410−418.
12. Pugh, E. N., Jr., and Lamb, T. D. (2000) in *Handbook of Biological Physics* (Stavenga, D. G., DeGrip, W. J., and Pugh, E. N., Jr., Eds.) pp 183−255, Elsevier Science B. V., North-Holland.
13. Burns, M. E., and Baylor, D. A. (2001) *Annu. Rev. Neurosci. 24*, 779−805.

14. Fain, G. L., Matthews, H. R., Cornwall, M. C., and Koutalos, Y. (2001) *Physiol. Rev. 81*, 117−151.
15. Franco, M., Chardin, P., Chabre, M., and Paris, S. (1996) *J. Biol. Chem. 271*, 1573−1578.
16. Goldberg, J. (1998) *Cell 95*, 237−248.
17. McLaughlin, S., and Aderem, A. (1995) *Trends Biochem. Sci. 20*, 272−276.
18. Ames, J. B., Tanaka, T., Stryer, L., and Ikura, M. (1996) *Curr. Opin. Struct. Biol. 6*, 432−438.
19. Zozulya, S., and Stryer, L. (1992) *Proc. Natl. Acad. Sci. U.S.A. 89*, 11569−11573.
20. Dizhoor, A. M., Chen, C.-K., Olshevskaya, E., Sinelnikova, V. V., Phillipov, P., and Hurley, J. B. (1993) *Science 259*, 829−832.
21. Kawamura, S., Hisatomi, O., Kayada, S., Tokunaga, F., and Kuo, C.-H. (1993) *J. Biol. Chem. 268*, 14579−14582.
22. Senin, I. I., Zargarov, A. A., Alekseev, A. M., Gorodovikova, E. N., Lipkin, V. M., and Philippov, P. P. (1995) *FEBS Lett. 376*, 87−90.
23. Olshevskaya, E. V., Hughes, R. E., Hurley, J. B., and Dizhoor, A. M. (1997) *J. Biol. Chem. 272*, 14327−14333.
24. Schrem, A., Lange, C., Beyermann, M., and Koch, K.-W. (1999) *J. Biol. Chem. 274*, 6244−6249.
25. Otto-Bruc, A., Buczylko, J., Surgucheva, I., Subbaraya, I., Rudnicka-Nawrot, M., Crabb, J. W., Arendt, A., Hargrave, P. A., Baehr, W., and Palczewski, K. (1997) *Biochemistry 36*, 4295−4302.
26. Sokal, I., Alekseev, A., Baehr, W., Haeseleer, F., and Palczewski, K. (2002) *Biochemistry 41*, 251−257.
27. Krylov, D. M., Niemi, G. A., Dizhoor, A. M., and Hurley, J. B. (1999) *J. Biol. Chem. 274*, 10833−10839.
28. Hwang, J.-Y., and Koch, K.-W. (2002) *Biochim. Biophys. Acta* (in press).
29. Tsien, R., and Pozzan, T. (1989) *Methods Enzymol. 172*, 230−262.
30. Schoenmakers, T. J. M., Visser, G. J., Flik, G., and Theuvenet, A. P. R. (1992) *BioTechniques 12*, 870−879.
31. Martell, A. E., and Smith, R. M. (1974) *Critical stability constants*, Plenum Press, New York.
32. Wiegand, R. D., and Anderson, R. E. (1982) *Methods Enzymol. 81*, 297−304.
33. Lange, C., and Koch, K.-W. (1997) *Biochemistry 36*, 12019−12026.
34. Hwang, J.-Y., Schlesinger, R., and Koch, K.-W. (2001) *FEBS Lett. 508*, 355−359.
35. Béven, L., Adenier, H., Kichenama, R., Homand, J., Redeker, V., Le Caer, J.-P., Ladant, D., and Chopineau, J. (2001) *Biochemistry 40*, 8152−8160.
36. Rudnicka-Nawrot, M., Surgucheva, I., Hulmes, J. D., Haeseleer, F., Sokal, I., Crabb, J. W., Baehr, W., and Palczewski, K. (1998) *Biochemistry 37*, 248−257.
37. Sokal, I., Otto-Bruc, A. E., Surgucheva, I., Verlinde, C. L. M. J., Wang, C.-K., Baehr, W., and Palczewski, K. (1999) *J. Biol. Chem. 274*, 19829−29837.
38. Hughes, R. E., Brzovic, P. S., Dizhoor, A. M., Klevit, R. E., and Hurley, J. B. (1998) *Protein Sci. 7*, 2675−2680.
39. Tanaka, T., Ames, J. B., Harvey, T. S., Stryer, L., and Ikura, M. (1995) *Nature 376*, 444−447.
40. Ames, J. B., Ishima, R., Tanaka, T., Gordon, J. I., Stryer, L., and Ikura, M. (1997) *Nature 389*, 198−202.
41. Ames, J. B., Dizhoor, A. M., Ikura, M., Palczewski, K., and Stryer, L. (1999) *J. Biol. Chem. 274*, 19329−19337.
42. Ermilov, A. N., Olshevskaya, E. V., and Dizhoor, A. M. (2001) *J. Biol. Chem. 276*, 48143−48148.
43. Dizhoor, A. M., and Hurley, J. B. (1996) *J. Biol. Chem. 271*, 19346−19350.
44. Mendez, A., Burns, M., Sokal, I., Dizhoor, A. M., Baehr, W., Palczewski, K., Baylor, D. A. and Chen, J. (2001) *Proc. Natl. Acad. Sci. U.S.A. 98*, 9948−9953.
45. Howes, K. A., Pennesi, M. E., Sokal, I., Church-Kopish, J., Schmidt, B., Margolis, D., Frederick, J. M., Rieke, F., Palczewski, K., Wu, S. M., Detwiler, P. B., and Baehr. W. (2002) *EMBO J. 21*, 1545−1554.
46. O'Callaghan, D. W., Ivings, L., Weiss, J. L., Ashby, M. C., Tepikin, A. V., and Burgoyne, R. D. (2002) *J. Biol. Chem. 277*, 14227−14237.
47. Vijay-Kumar, S., and Kumar, V. D. (1999) *Nat. Struct. Biol. 6*, 80−88.
48. Bourne, Y., Dannenberg, J., Pollmann, V., Marchot, P., and Pongs, O. (2001) *J. Biol. Chem. 276*, 11949−11955.

BI026618Y